

## 2-5-4 Calibration of EMI Antennas for Microwave Frequency Bands by the Extrapolation Technique

Katsumi FUJII, Kojiro SAKAI, Tsutomu SUGIYAMA, Kouichi SEBATA, and Iwao NISHIYAMA

Two calibration methods with the extrapolation technique are proposed to calibrate the actual gain for EMI antennas above 1 GHz. In this method, the  $S_{21}$  at the infinite distance between antennas are estimated from the  $S_{21}$  values measured at near-field region by means of the least squares method. The calibration results of two kinds of double-ridged guide antennas (DRGAs) were compared with those calibrated in a large full anechoic chamber. It shows that the accuracy of the proposed methods depends on the directivity of the antenna under calibration and that the methods can yield the actual gain with an error less than  $\pm 1.0$  dB for almost all frequency even at a small semi-anechoic chamber with a metal ground plane.

### 1 Introduction

With the increasingly higher operation frequency of the computers integrated in electric/electronic instruments, the need for measuring spatial radiation from these devices, electromagnetic interference (EMI), has become increasingly urgent. In line with this trend, a CIPSR (Comité international spécial des perturbations radioélectriques) regulation on the allowance level and measurement method of radiation noise at high frequencies ( $\geq 1$  GHz) has accepted as international standard [1]. In Japan, a VCCI regulation (applicable to the frequency range from 1 to 6 GHz) entered into force in Oct. 2010 [2]. This regulation stipulates the use of linearly polarized wave antennas for EMI measurement: the most widely used types include: DRGA (Double-ridged guide antenna) and LPDA (Log-periodic dipole array antenna) (see Fig. 1). These are especially suited for EMI measurement because of the wide frequency coverage (1–18 GHz) with a single antenna.

As a prerequisite for EMI measurement, knowledge of basic parameters — antenna factor and actual gain — is essential. To determine these parameters, two calibration methods — the three-antenna method and the reference antenna method (see Subsection 3.2) — are used: radio propagation characteristics between transmitting and receiving antennas are measured in a fully anechoic room.

However, the calibration of DRGA, LPDA, and other antennas that extend in one direction, using the three-antenna method, may produce different results depending on the definition of distance between antennas (i.e. which

spatial point of the transmitting and which spatial point of the receiving antenna are counted for the antenna distance). In addition, the reference antenna method also has an issue: in the case where the shape of the standard antenna (STD) and the antenna under calibration (AUC) do not coincide, calibration may give discrepancies depending on the parts of the antennas that were replaced.

One way to resolve such problems is to ensure a large enough distance between the transmitting- and receiving antennas, so that their size becomes negligible. Generally, however, it is a tall order to provide such a large fully anechoic room that accommodates a very long distance between antennas. Some researchers have proposed the use of an open area test site for calibration [3][4], but it is more convenient if calibration can be performed in a fully anechoic room with a size comparable to that used in EMI measurements.

For antennas with relatively simple structures, several methods have been proposed to correct the measured results gained using the short distance between antennas with theoretical calculations and simulation results [5][6]. Other methods have also been proposed to correct the distance between antennas, in which an apparent radiation point (phase center) is calculated for use in the correction [7]–[9]. These corrective methods, however, pose problems regarding the validity of theoretical calculations and numerical simulations. The more complex the antenna structure becomes, the more difficult it becomes to accurately evaluate detailed size measurements for data input. Numerical simulations may produce differences in outcome depend-

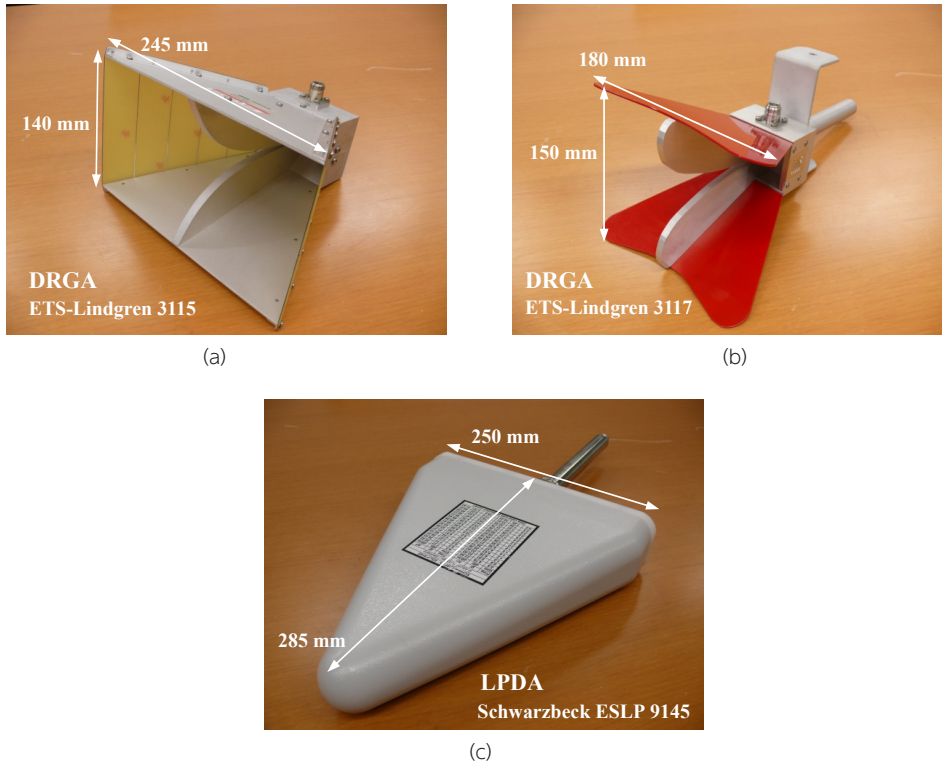


Fig. 1 EMI antennas used for microwave bands

ing on the modeling method, and on the number of segmentations. For example, the antenna shown in Fig. 1 (c) defies numerical simulation because its invisible element structure makes it practically impossible to gain detailed size measurements. An attempt to determine the phase center from measurements requires a sufficient distance between antennas, rendering the need for a large fully anechoic room.

In this paper, we examine the validity of a method to determine the actual gain of antennas, which is capable of being conducted in a small anechoic chamber with a comparable size to that used in EMI measurements. In specific terms, the S-parameter ( $S_{21}$ ) between the transmitting- and receiving antennas is measured at different distances to evaluate distance properties, to which an extrapolation technique is applied to estimate the value at an infinitely large distance between antennas. Actual gain can be calculated from this value [10].

## 2 Actual gain and antenna factor

The gain of an antenna is defined as the ratio of two power density values, e.g. the power density of radiation emitted toward a given direction from the antenna under calibration, and that from the standard antenna [11]. The ratio is called “absolute gain” if the standard antenna used

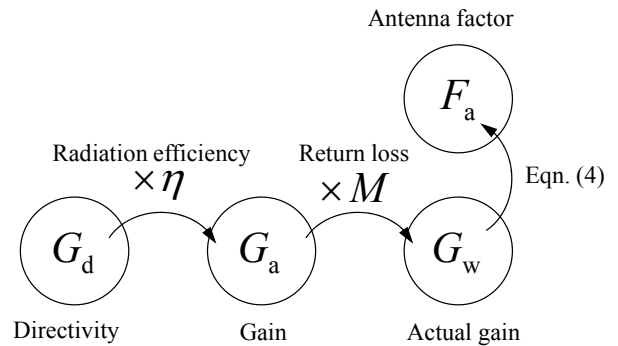


Fig. 2 Relations connecting gain to antenna factor

is of isotropic emission characteristic, and “relative gain” in other cases. For relative gain measurements, half-wave dipole antennas are often used as the standard antenna. Other measures include directivity, which is calculated based on the total energy emitted in all directions from the antenna, and “actual gain” which takes mismatching factors between the antenna and feeder line into consideration.

Gain ( $G_a$ ), directivity ( $G_d$ ), and actual gain ( $G_w$ ) are mutually correlated as shown in the following equations, where  $\eta$  and  $M$  represent the radiation efficiency and return loss, respectively. Mutual relationships among them are also shown schematically in Fig. 2.

$$G_w = G_a \frac{1}{M} = \eta G_d \frac{1}{M} \tag{1}$$

Where, the reflection loss  $M$  is expressed as:

$$M = \frac{1}{1 - |\Gamma_{in}|^2} \quad (2)$$

And,  $\Gamma_{in}$  represents the reflection coefficient of the antenna defined by the following equation.

$$\Gamma_{in} = \frac{Z_{in} - Z_0}{Z_{in} + Z_0} \quad (3)$$

Where,  $Z_{in}$  represents the input impedance of the antenna, and  $Z_0$  represents the characteristic impedance of the power feeder line to the antenna (real value). If the antenna is loss-free (100% radiation efficiency), and with perfect impedance matching ( $\Gamma_{in}=0$ ), the three values, actual gain, gain, and directivity, all coincide.

In view of the fact that the majority of actual EMI measurements are made using  $Z_0 = 50 \Omega$  coaxial cables and measuring devices, the following paragraphs describe the method to determine actual gain at  $Z_0 = 50 \Omega$  (the standard antenna is assumed to be isotropic).

At  $Z_0 = 50 \Omega$ , the relation between active gain and antenna factor ( $F_a$ ) is expressed as follows [11]-[13].

$$F_a = \left( \frac{2\pi}{\lambda} \right) \sqrt{\frac{120}{G_w Z_0}} \quad (4)$$

Normally, active gain and antenna factor are expressed in dB. Therefore, by taking the common logarithm of both sides, and then multiplying them by 20, the following relation is obtained.

$$F_a \text{ [dB(1/m)]} = G_w \text{ [dBi]} + 20 \log_{10} f_{\text{GHz}} + 30.22 \quad (5)$$

Where,  $f_{\text{GHz}}$  is the frequency represented in GHz. By using the antenna coefficient, as in the case of EMI measurement in the range below 1 GHz, reception field strength  $E$  can be determined by substituting the received voltage  $V$  in the following relation.

$$E \text{ [dB(\mu V/m)]} = F_a \text{ [dB(1/m)]} + V \text{ [dB}_{\mu}\text{]} \quad (6)$$

### 3 Calibration in far field

The calibration methods applicable in cases in which the distance between the transmitting and receiving antennas is large enough are described in [14]. In recent years, a vector network analyzer (VNA) is often employed for calibration, typically for  $S_{21}$  measurement between the transmitting and receiving antennas. This paper assumes calibration that involves  $S_{21}$  measurement, and lists and describes the equations required. In conventional calibration that employs both a signal generator and receiver, substitutions of  $P_0$  and  $P_1$  into the following equation gives  $S_{21}$ .

$$|S_{21}| = 10 \log_{10} \frac{P_1}{P_0} \Big|_{\Gamma_G = \Gamma_L = 0} \quad (7)$$

Where,  $P_0$  represents the received power through direct connection, and  $P_1$  represents the received power through radio wave transmission (i.e. transmitting and receiving antennas are connected). This equation holds only if the following conditions are satisfied: reflection from the signal generator ( $\Gamma_G$ ) and receiver ( $\Gamma_L$ ) are both zero, and the characteristics (loss) of the adaptor used for direct cable connection are properly compensated.

#### 3.1 Reference antenna method

The reference antenna method is a generally and widely used antenna calibration technique, in which the AUC (antenna under calibration for determining actual gain ( $G_w$ )) is replaced by the STD with known  $G_w$  (STD) for comparative measurements. The STD has been calibrated in a superior calibration laboratory and its actual gain is written in the certification ("calibration certification," "calibration results," etc.). In VNA-based calibration procedures (see Fig. 3),  $S_{21}$ (STD) is first measured by placing STD at a sufficiently large distance from the transmitting antenna, and then the STD is replaced by AUC for  $S_{21}$ (AUC) measurement. Actual gain,  $G_w$ (AUC), can be determined by comparing these two values.

$$G_w \text{ (AUC)} = G_w \text{ (STD)} \frac{|S_{21} \text{ (AUC)}|^2}{|S_{21} \text{ (STD)}|^2} \quad (8)$$

Measurements are taken normally in dB. In this case, the multiplications become simple addition operations.

$$G_w^{\text{dB}} \text{ (AUC)} = G_w^{\text{dB}} \text{ (STD)} + S_{21}^{\text{dB}} \text{ (AUC)} - S_{21}^{\text{dB}} \text{ (STD)} \quad [\text{dBi}] \quad (9)$$

In Figure 3, STD and AUC are replaced in a way so that the aperture surfaces of the two antennas coincide. In many cases, however, the apertures differ in form, producing a configuration problem as to what portion of these antennas should coincide spatially. Even if the STD and AUC have a common shape, this fortunate situation does not guarantee that the distance between antennas is sufficient: an inappropriate distance setting may lead to uncertain results. A well-known criterion for achieving far-field condition is a distance between antennas of  $2D^2/\lambda$ , where  $D$  is the antenna aperture diameter, and  $\lambda$  is the wavelength. However, it varies depending on such factors as the shape of the antenna and required level of uncertainty. For example, even if the two antennas have common aperture size  $D$ ,

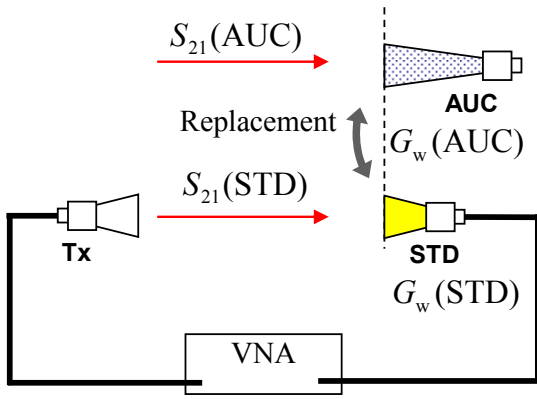


Fig. 3 Reference antenna method

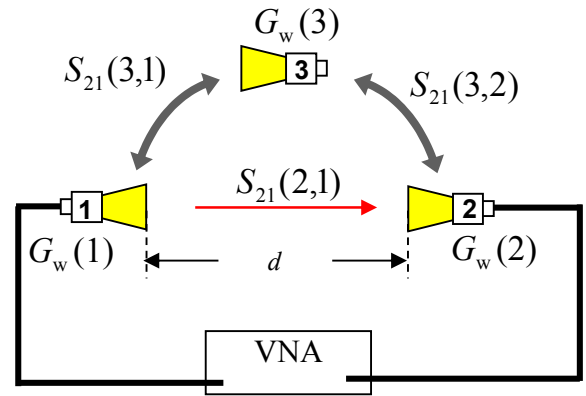


Fig. 4 Three-antenna method

differences in size and shape along the transmission direction make additional considerations necessary for optimum results.

### 3.2 Three-antenna method

The three-antenna method is characterized by using three antennas, all with unknown actual gain, to determine the three actual gain values simultaneously. To achieve this goal,  $S_{21}$  measurements are made between the transmitting and receiving antennas in three combinations of the antennas. As shown in Fig. 4, two antennas are selected out of the three, one for transmitting and one for receiving, to measure  $S_{21}$  between them.

From the three measurements thus performed, the actual gain for antenna #1, for example, is determined using the following equation.

$$G_w(1) = \frac{4\pi d}{\lambda} \sqrt{\frac{|S_{21}(2,1)|^2 |S_{21}(3,1)|^2}{|S_{21}(3,2)|^2}} \quad (10)$$

Where,  $S_{21}(j, i)$  means the  $S_{21}$  as determined when radio waves are transmitted from antenna #i to antenna #j.

Measurements are taken normally in dB. In this case, the multiplications become simple addition operations.

$$G_w^{dB}(1) = 16.22 + 10 \log_{10} f_{GHz} + 10 \log_{10} d + \frac{1}{2} \{ S_{21}^{dB}(2,1) + S_{21}^{dB}(3,1) - S_{21}^{dB}(3,2) \} \quad (11)$$

Where, the following relation is utilized, and  $c$  represents the speed of light.

$$\begin{aligned} 10 \log_{10}(4\pi/\lambda) &= 10 \log_{10}(4\pi/c \cdot 10^9) + 10 \log_{10} f_{GHz} \\ &= 16.22 + 10 \log_{10} f_{GHz} \end{aligned} \quad (12)$$

The third term in the right side of Equation (11) indicates that the calculation needs input of distance between antennas  $d$ . The distance between antennas,  $d$ , in Fig. 4 is il-

lustrated simply as the between apertures. In actual situations, however, there is always ambiguity as to how  $d$  should be defined — i.e. from which part of the transmitting to which part of receiving antenna. The  $d$  is defined often as distance between apertures in view of convenience of measurement operations, but this may result in biased actual gain and uncertainties in calibration results.

## 4 Estimation of propagation characteristics by means of extrapolation

For antennas with spatial extension along the direction of transmission, as described up to this point, improper setting of the distance between antennas,  $d$ , may produce doubtful results. As a solution to this problem, an estimation method by extrapolation has been proposed and is adopted in national standardization organizations for metrology around the world. In this method, transmission characteristics at infinity are extrapolated based on the distance characteristics determined based on the  $S_{21}$  measurements taken at relatively small distance between antennas.

Let us consider taking  $S_{21}$  measurements using the configuration shown in Fig. 5 (a), in which a pair of transmitting and receiving antennas are facing each other at a relatively small distance. Four ports are defined as follows: port #0; transmitting antenna's connector, port #1; a plane at the aperture position of the transmitting antenna, port #2; a plane set up at the aperture position of the receiving antenna, and port #3; receiving antenna's connector. When  $S_{21}$  measurements are taken using VNA, it gives distance characteristics between port #0 and port #3. Note here that that the positions of port #1 and port #2 do not need to exactly coincide with the aperture surface of the antennas: for example, the distance  $d$  may be the

interval between the two reference markings that indicate the distance between antennas. Figure 5 (b) is a signal flow diagram illustrating how the signal flows from port #0 to port #3.

Where, T and R represent characteristics of the transmitting and receiving antennas, respectively. Taking multiple reflections into consideration,  $S_{21}$  can be expressed using the following equation [10].

$$S_{21}(d) = \sum_{m=0}^{\infty} \frac{e^{-j(2m+1)kd}}{d^{2m+1}} \sum_{n=0}^{\infty} A_{mn} d^{-n} \\ = \frac{e^{-jkd}}{d} \left( A_{00} + \frac{A_{01}}{d} + \frac{A_{02}}{d^2} + \dots \right) + \frac{e^{-j3kd}}{d^3} \left( A_{10} + \frac{A_{11}}{d} + \frac{A_{12}}{d^2} + \dots \right) + \dots \quad (13)$$

In view of the property of spatial propagation characteristic (between port #1 and port #2) that it is inversely proportional to  $d$ , this relation can be transformed into the following format by multiplying both sides by  $d$ , and then by taking the square.

$$|S_{21}(d) \cdot d|^2 = A_0 + A_1 \left( \frac{1}{d} \right) + A_2 \left( \frac{1}{d} \right)^2 + A_3 \left( \frac{1}{d} \right)^3 + \dots \quad (14)$$

The first constant term  $A_0$  on the right side is the product of T and R squared (both are characteristic values of transmitting and receiving antennas), indicating that it does not depend on the distance.

$$\lim_{d \rightarrow \infty} |S_{21}(d) \cdot d|^2 = A_0 = |T|^2 |R|^2 \quad (15)$$

The value of the constant  $A_0$  can be determined by extending the distance between antennas  $d$  to infinity, which is, however, impossible in actual situations. We have to estimate the value from measurements performed at finite distance between antennas. To achieve this goal, we consider the following polynomial and apply least square regression fitting using a series of  $S_{21}(d)$  data measured at a different distance between antennas,  $d$ .

$$f\left(\frac{1}{d}\right) = A_0 + A_1 \left( \frac{1}{d} \right) + A_2 \left( \frac{1}{d} \right)^2 + A_3 \left( \frac{1}{d} \right)^3 + \dots \quad (16)$$

Figure 6(b) shows an example of measured results. In this example, measurements were taken at 3 GHz, and at a series of inter-aperture surface distances  $d$ . The experiment used the same type of antenna (ETS-Lindgren: type 3115), see Fig. 1 (a), for both the transmitting and receiving antenna. The measured values are plotted against  $|S_{21}(d) \cdot d|^2$  (vertical axis) and  $(1/d)$  (horizontal axis), and the polynomial shown in Equation (16) is fitted to this plot while changing its order. The distance between antennas is smaller as the graph approaches the right end and greater as it approaches the left end. Therefore, the search for  $A_0$  at an infinitely large distance between antennas is equivalent

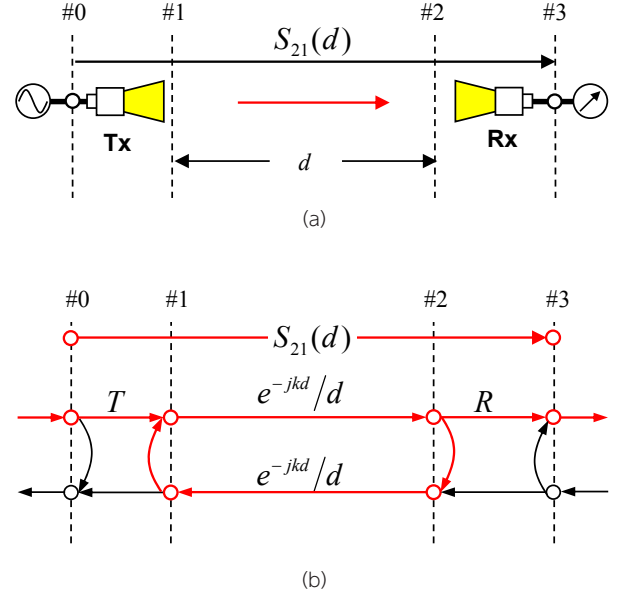


Fig. 5 Propagation model between antennas

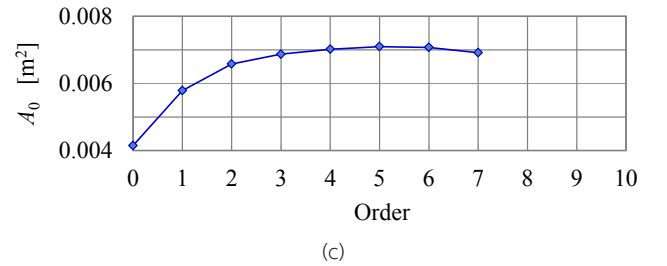
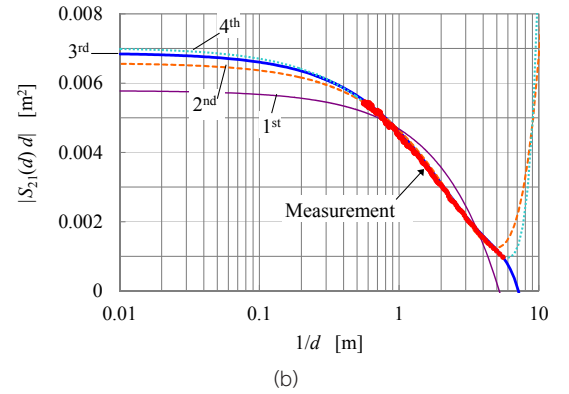
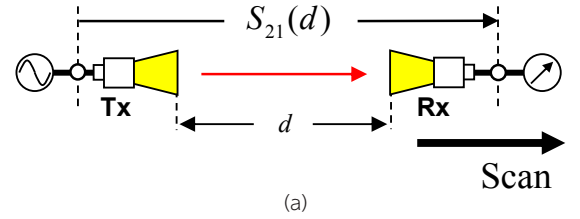


Fig. 6 Distance characteristics of  $S_{21}$  and dependency of  $A_0$  on the order of regression curve

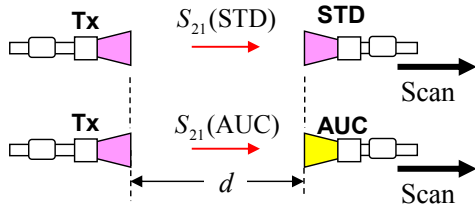


Fig. 7 Reference antenna method with extrapolation technique

lent to calculating the intercept of the regression curve. As seen from Fig. 6 (b), each regression curve tends to converge to a constant value as it moves to the left (greater distance between antennas). One problem here is the selection of polynomial order for obtaining the optimum regression model. The selection depends on such factors as the shape of the antenna, measurement frequency, and the settings of the distance between antennas for obtaining data (higher order is required as the distance becomes smaller). F-test [10] and AIC [15] may be useful for determining the order. Another approach is to select the order that minimizes uncertainty of calibration [16][17]. Figure 6 (c) indicates that the  $A_0$  value converges as the order of regression curve increases. As seen from this plot, for the specific antenna pair that features distance characteristics shown in Fig. 6 (b), a third order polynomial gives sufficient accuracy. Note that a too-high polynomial order may cause the regression curve to behave peculiarly, resulting in a dubious  $A_0$  value.

**4.1 Reference antenna method based on extrapolation technique**

Two sets of distance dependency data for  $S_{21}$  are measured — one between the transmitting antenna and STD, and the other between the transmitting antenna and AUC (see Fig. 7) — and  $A_0(\text{STD})$  and  $A_0(\text{AUT})$  are estimated respectively by extrapolation technique. The actual gain of the AUC is obtained by substituting these two values into the equation below.

$$G_w(\text{AUC}) = G_w(\text{STD}) \frac{A_0(\text{AUC})}{A_0(\text{STD})} \tag{17}$$

Where,

$$A_0 = \lim_{d \rightarrow \infty} |S_{21}(d) \cdot d|^2$$

Equation (17) can be rewritten as follows, if the values are expressed in dB.

$$G_w^{\text{dB}}(\text{AUC}) = G_w^{\text{dB}}(\text{STD}) + A_0^{\text{dB}}(\text{AUC}) - A_0^{\text{dB}}(\text{STD}) \tag{18}$$

[dB]

Where,

$$A_0^{\text{dB}} = 20 \log_{10} A_0$$

This is equivalent to situation where the STD and AUC replacements take place at infinitely separated locations from the transmitting antenna. Therefore, the effects caused by positional errors, as described in 3.1, do not occur.

**4.2 Three-antenna method with extrapolation technique**

A generalized version of three-antenna method, which is applicable even if one of the three is a circularly-polarized antenna, is described in references [10]. There are many cases, however, where it is apparent that all of the three are linearly-polarized antennas. In such cases, the following equations can determine the actual gain using the measurements gained from a simplified experimental configuration (see Fig. 8), in which the antennas are so arranged that their planes of polarization coincide.

$$G_w(1) = \frac{4\pi}{\lambda} \sqrt{\frac{A_0(2,1)A_0(3,1)}{A_0(3,2)}} \tag{19-1}$$

$$G_w(2) = \frac{4\pi}{\lambda} \sqrt{\frac{A_0(2,1)A_0(3,2)}{A_0(3,1)}} \tag{19-2}$$

$$G_w(3) = \frac{4\pi}{\lambda} \sqrt{\frac{A_0(3,1)A_0(3,2)}{A_0(2,1)}} \tag{19-3}$$

Where,

$$A_0(j,i) = \lim_{d \rightarrow \infty} |S_{21}(j,i) \cdot d|^2, (j,i) = (2,1), (3,1), (3,2)$$

If the measurements are expressed in dB, the equations can be rewritten as:

$$G_w^{\text{dB}}(1) = 16.22 + 10 \log_{10} f_{\text{GHz}} + \frac{1}{2} \{ A_0^{\text{dB}}(2,1) + A_0^{\text{dB}}(3,1) - A_0^{\text{dB}}(3,2) \} \tag{20-1}$$

[dBi]

$$G_w^{\text{dB}}(2) = 16.22 + 10 \log_{10} f_{\text{GHz}} + \frac{1}{2} \{ A_0^{\text{dB}}(2,1) - A_0^{\text{dB}}(3,1) + A_0^{\text{dB}}(3,2) \} \tag{20-2}$$

[dBi]

$$G_w^{\text{dB}}(3) = 16.22 + 10 \log_{10} f_{\text{GHz}} + \frac{1}{2} \{ -A_0^{\text{dB}}(2,1) + A_0^{\text{dB}}(3,1) + A_0^{\text{dB}}(3,2) \} \tag{20-3}$$

[dBi]

Where,

$$A_0^{\text{dB}}(j,i) = 20 \log_{10} A_0(j,i) \quad (j,i) = (2,1), (3,1), (3,2)$$

It is easy to see that these sets of Equations (19) and (20) do not contain any distance term  $d$ , indicating that the problems involving the distance between antennas are eliminated.

## 5 Calibration results

In this section, some of the calibration results gained from the “reference antenna method with extrapolation technique” and the “three-antenna method with extrapolation technique” are presented to illustrate the validity of these techniques. In all the experiments, two types of DRGA (ETS-Lindgren type 3115 and 3117; see Fig. 1) are operated at a range of frequencies from 1 GHz to 18 GHz.

The calibrations were performed in a semi-anechoic chamber (internal dimensions: 8 m (L) × 6 m (W) × 5.5 m (H)) without covering the ground plane with radio wave absorbers as shown in Fig. 9. The transmitting and receiving antennas are set at the height  $h = 2$  m, configured for horizontally-polarized wave measurements, and distance between antennas ( $d$ : between the aperture planes) were adjusted in the range from 6 cm to 4 m at 1 cm increments using an antenna positioner. The  $S_{21}$  measurements were taken using a network analyzer (VNA) that had been calibrated by the SOLT calibration method.

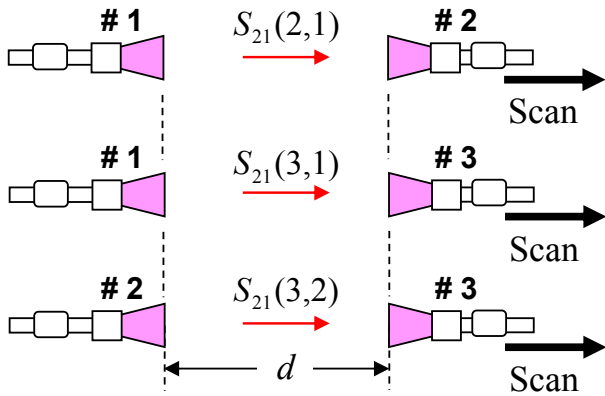


Fig. 8 Three-antenna method with extrapolation technique

In reference [10], an antenna sweeping range from  $0.2(a^2/\lambda)$  to  $2(a^2/\lambda)$  is recommended, where  $a$  represents the aperture diameter of the antenna. Assuming  $a=30$  cm (aperture diameter of the two DRGAs used in this paper), the distance between antennas (between the aperture planes) was determined as shown in Table 1.

Note that the maximum distance was limited to 4 m, and the values shown in parentheses in Table 1 indicate those recommended in reference [10]. The maximum scan distances meet the recommended values up to the frequency 6 GHz, but fall short of going beyond them. We decided to use the following 3rd order polynomial as the regression model in all cases.

$$f\left(\frac{1}{d}\right) = A_0 + A_1\left(\frac{1}{d}\right) + A_2\left(\frac{1}{d}\right)^2 + A_3\left(\frac{1}{d}\right)^3 \quad (21)$$

### 5.1 Calibration using the reference antenna method with extrapolation technique

In the experiments carried out in a large fully anechoic room, DRGA3117 was used as the STD, which had been calibrated using Equation (11) — the distance between the transmitting and receiving antennas (one aperture plane to the other) was assumed to be 15.1 m. DRGA 3117

Table 1 Antenna scanning distance

Values in parentheses indicate those recommended in reference [10]

Freq. GHz	Starting distance m	Ending distance m
1	0.06	0.6
3	0.18	1.8
6	0.36	3.6
9	0.54	4.0 (5.4)
12	0.72	4.0 (7.2)
15	0.90	4.0 (9.0)
18	1.08	4.0 (10.8)

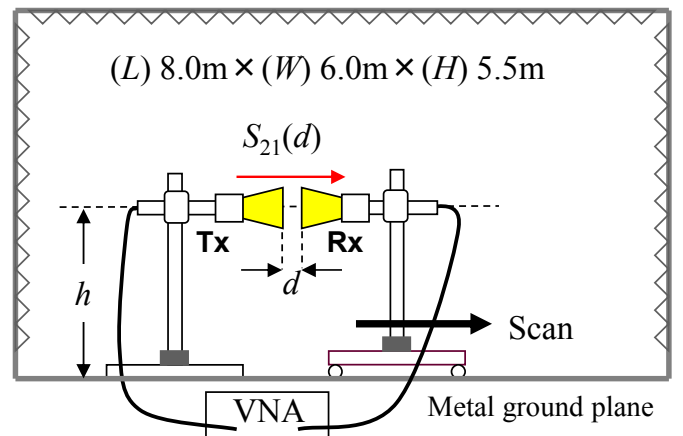
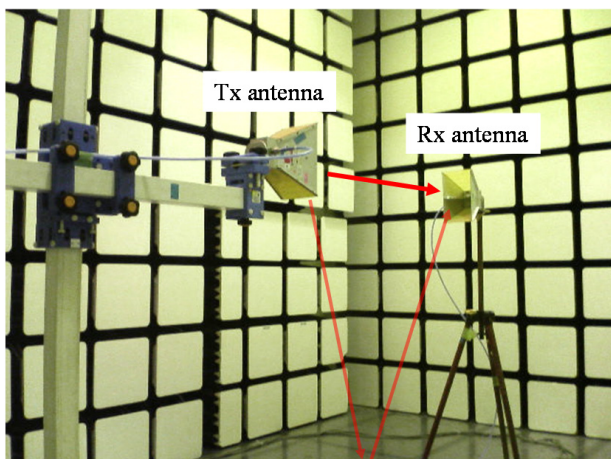
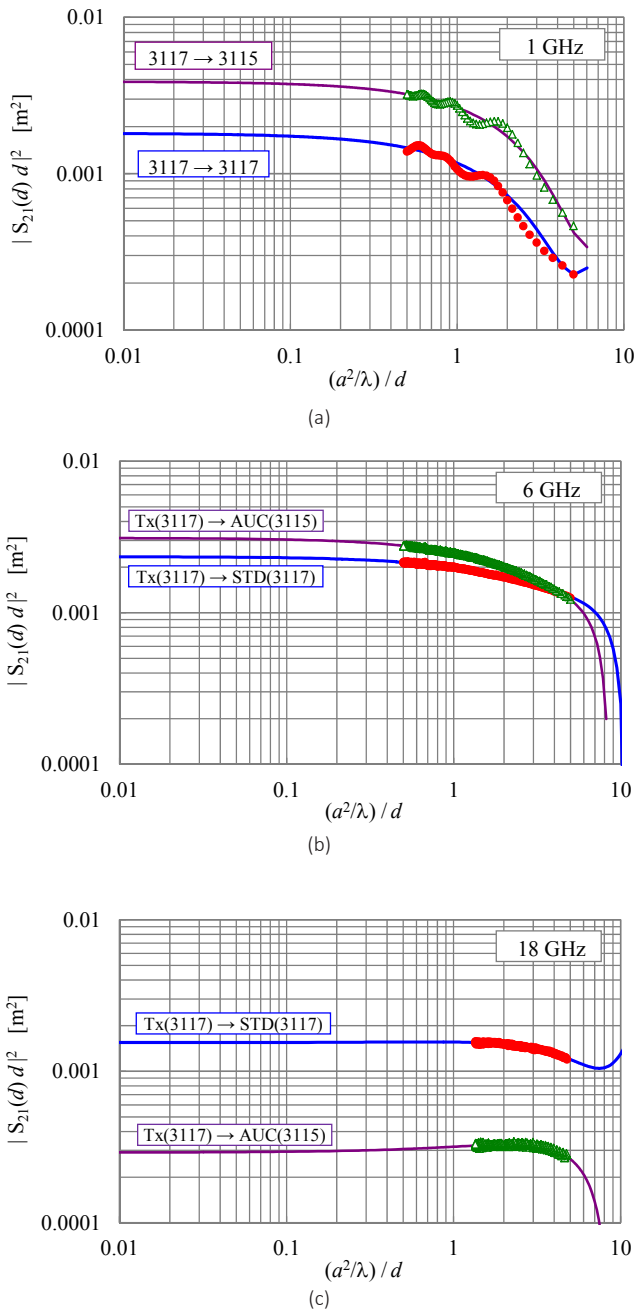


Fig. 9 Antenna calibration in a semi-anechoic chamber

was also used as the transmitting antenna. Figure 10 illustrates the measurement results obtained at 1 GHz, 6 GHz, and 18 GHz, where the horizontal axis represents  $(a^2/\lambda)$  and vertical axis  $|S_{21}(d) \cdot d|^2$ . The distance  $d$  indicates that between aperture planes. In this figure, the points shown in  $\bullet$  (red) and  $\triangle$  (green) represent the measured data, and the regression curve calculated from these data is plotted in a solid line. It can be seen that the value in the horizontal axis ( $|S_{21}(d) \cdot d|^2$ ) converges to a certain value (i.e.  $A_0$ ) as the distance  $d$  increases.

Actual gain can be determined from the set of  $A_0$  values



**Fig. 10** Measurement results of  $S_{21}$  and estimated  $A_0$  (reference antenna method)

obtained at each frequency (see Fig. 11). Actual gain thus calculated is shown in Fig. 11 (a), and comparison with the results from the large fully anechoic room experiment is shown in Fig. 11 (b).

In the case where DRGA 3115 is used as AUC as shown in  $\triangle$  (green), deviation becomes large at frequencies exceeding 14 GHz. The discrepancy can be ascribed to, in addition to insufficient sweep range, the following characteristic peculiar to DRGA 3115: it shows maximum directivity at different directions than its frontal direction. Due to this directivity characteristic, the effect of reflected waves from the surroundings has distance dependency, resulting in erroneous estimation of  $A_0$ . In contrast, in the experiments that use DRGA 3117 (with maximum directivity at its frontal direction) as AUC, interpolation from the measurement points ( $\bullet$  (red)) concludes correct actual gain values even in cases with a seemingly insufficient antenna sweeping extent.

In the experiments that used DRGA 3115, deviation becomes relatively large at the frequency range below 2 GHz. As is apparent from Fig. 10 (a), this deviation in

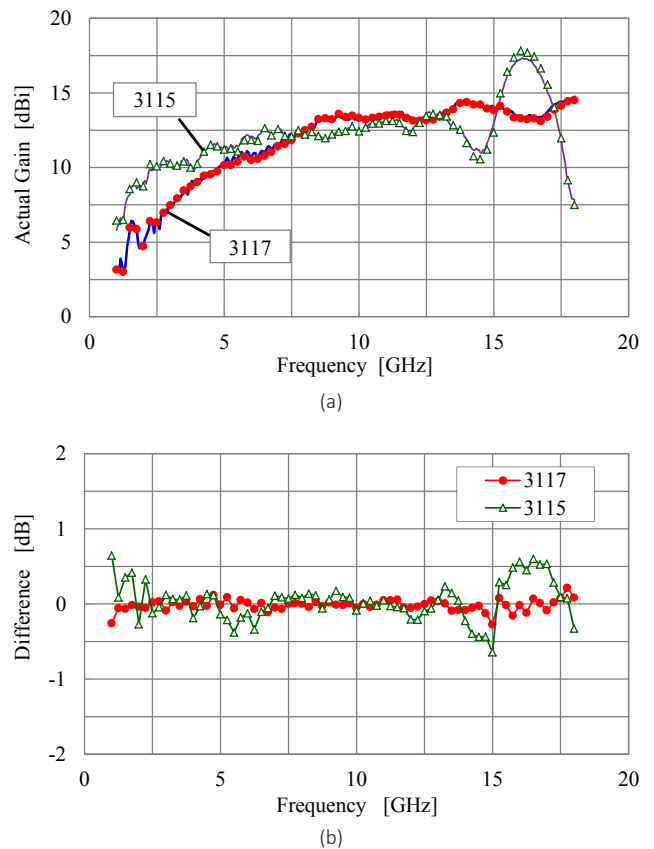


**Fig. 11** Calibration results of the reference antenna method with extrapolation technique  
(a) Actual gain, (b) Differences as compared with the results from large fully anechoic room experiments

estimation can be interpreted as due to the effect of multiple reflections between the transmitting and receiving antennas, and reflected waves from the ground plane. In addition, too small a number of measurement points may have exerted some effect. However, the experiments which used DRGA 3117 showed smaller deviation under the same conditions. This can be ascribed to the fact that STD and AUC are of the same shape, enabling them to cancel out various inadvertent effects.

From the results described above, in the case where

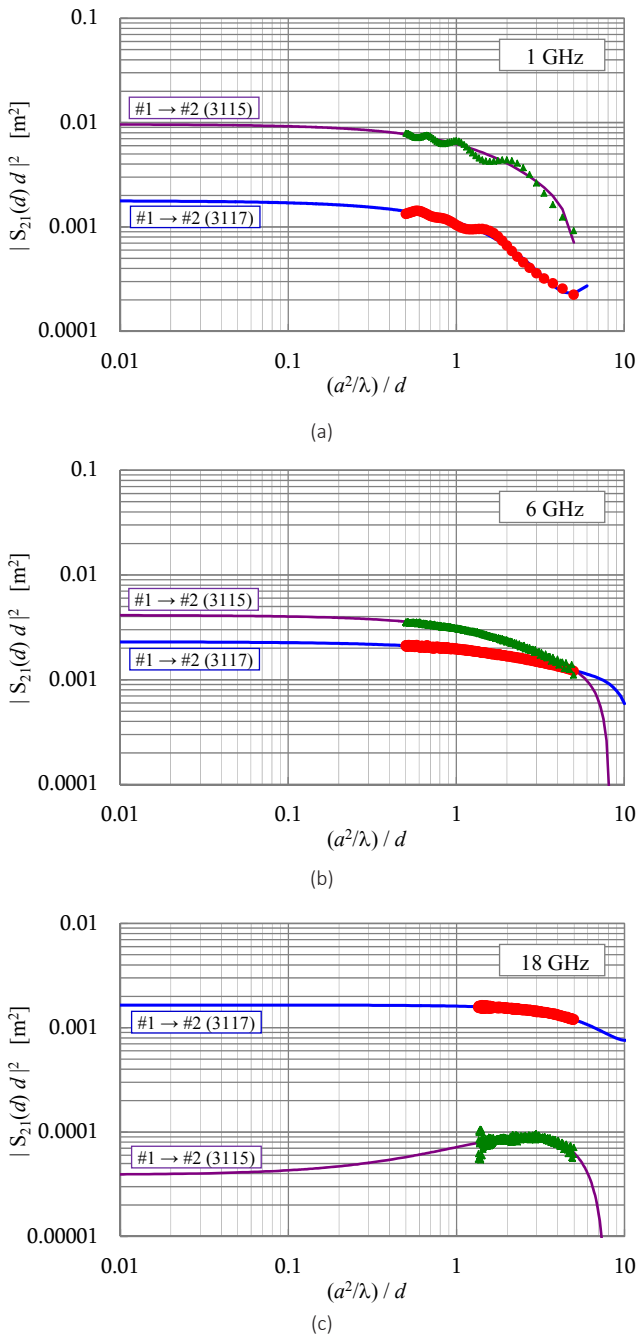


Fig. 12 Measurement results of  $S_{21}$  and estimated  $A_0$  (three-antenna method)

DRGA 3117 is used both as AUC and STD, calibration with extrapolation shows a good agreement with the those performed in a large fully anechoic room (within -0.3 dB and +0.2 dB in all frequencies). Also, the experiment that used DRGA 3115 showed agreement within -0.7 dB and +0.7 dB. If we focus on the narrower range between 1 and 6 GHz, the deviation falls within -0.3 and +0.1 dB for DRGA 3117 experiments, and within -0.4 and +0.7 dB for DRGA 3115 experiments.

### 5.2 Calibration using three-antenna method with extrapolation technique

Calibration using the three-antenna method with extrapolation technique was performed using combinations of three DRGA 3117s and three DRGA 3115s.

Figure 12 illustrates the measurement results obtained at 1 GHz, 6 GHz, and 18 GHz, where the vertical axis represent  $|S_{21}(d)d|^2$  and the  $A_0$  is evaluated from the experimental results (Fig. 13 shows the actual gain for antenna #1). The plots of points (● (red) and △ (green)) in Fig. 13 (a) indicate the results gained using extrapolation

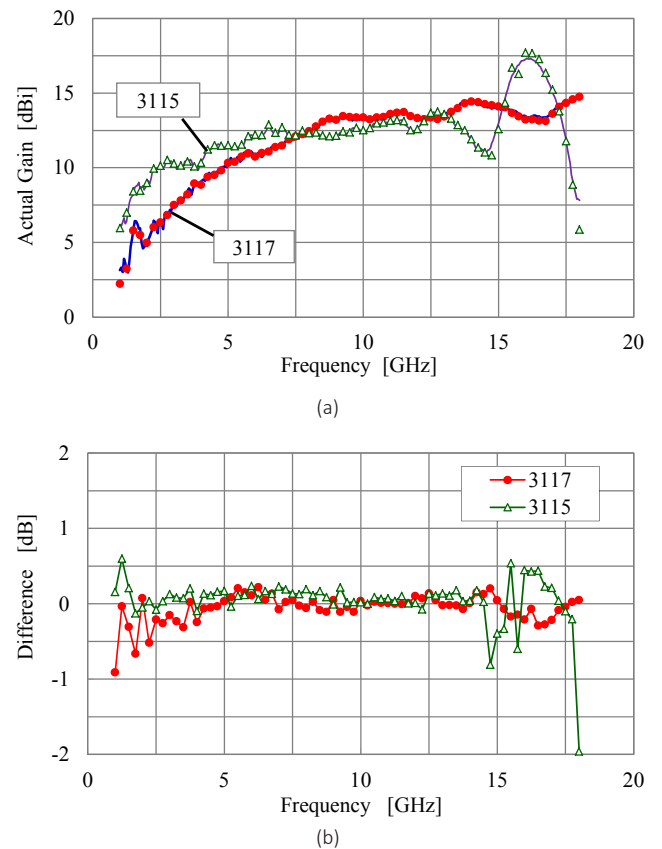


Fig. 13 Calibration results using three-antenna method with extrapolation technique

(a) Actual gain, (b) Differences as compared with the results from large fully anechoic room experiments

calculations, and the solid lines show the calibration results obtained in the large fully anechoic room - Equation (11) is used assuming the inter-aperture planes distance  $d = 15.1$  m. Figure 13 (b) plots deviation from the calibration results obtained in the large fully anechoic room. The deviation falls within the range between -0.5 to +0.5 dB for DRGA 3117, and -0.8 to +0.6 dB for DRGA 3115 except for the case with frequency 18 GHz. If we focus on the narrower range between 1 and 6 GHz, the deviation falls within -0.5 and +0.4 dB for DRGA 3117 experiments, and within -0.2 and +0.6 dB for DRGA 3115 experiments. The larger deviation observed at 18 GHz can be ascribed to insufficient sweeping distance as can be seen from Fig. 12 (c). Shorter sweeping distance, as compared to the cases with 1 GHz and 6 GHz, seems to hinder proper extrapolation, shifting the estimation of  $A_0$  too far on the smaller side.

### 6 Consideration of uncertainties

Uncertainties contained in the calibration results can be expressed by means of extended uncertainty estimation (level of confidence approx. 95 %), the magnitude of which is evaluated by synthesizing factors of uncertainty using Equations (22) and (23)[18]. In these equations, the magnitude of sensitivity is not explicitly written because they are all unity. Uncertainties of frequency are not written either, because they are known to be extremely small when compared with other uncertainty factors.

Uncertainty involved in the reference antenna method with extrapolation technique is evaluated using the following equation (synthesis of each uncertainty factors).

$$u(G_w^{dB}(AUC)) = \sqrt{u(G_w^{dB}(STD))^2 + u(A_0^{dB}(AUC))^2 - u(A_0^{dB}(STD))^2} \tag{22}$$

Where,

- $u(G_w^{dB}(AUC))$  : Uncertainty of AUC  $G_w$
- $u(G_w^{dB}(STD))$  : Uncertainty of STD  $G_w$
- $u(A_0^{dB}(AUC))$  : Uncertainty of  $A_0$  involved in AUC-transmitting antenna combination
- $u(A_0^{dB}(STD))$  : Uncertainty of  $A_0$  involved in STD-transmitting antenna combination

Uncertainty involved in  $G_w$  of the three-antenna method with extrapolation is evaluated by synthesizing uncertainty factors using the following equation. This equation technique is commonly applicable to antenna #1 to antenna #3.

$$u(G_w^{dB}) = \frac{1}{2} \sqrt{u(A_0^{dB}(2,1))^2 + u(A_0^{dB}(3,1))^2 + u(A_0^{dB}(3,2))^2} \tag{23}$$

Where,

- $u(A_0^{dB}(j,i))$  : Uncertainty of  $A_0$  associated with antenna #i and antenna #j combination

The values evaluated using Equations (22) and (23) are standard uncertainty: extended uncertainty (level of confidence approx. 95 %) is normally used for expressing uncertainty, which is calculated by multiplying a coverage factor  $k=2$ .

In the reference antenna method, as well as in the three-antenna method, uncertainty contained in  $A_0$  estimation propagates in the process of actual gain evaluation.

For both methods — the reference antenna method that includes the process of enlarging distance between antennas, and the three-antenna method — the factors affecting the uncertainty of  $A_0$  evaluation include: performance of VNA, effect of unwanted reflected waves from the surrounding environment, effect of deviation from the planned antenna positions, repeatability and reproducibility. In addition, uncertainty evolving from the use of extrapolation technique needs to be considered. In specific terms, such factors as positional deviation due to moving the antenna and sweeping, twisting and extending of the cables, and the use of least-square method to determine the regression curve can add uncertainties. These are the new factors to be considered that are not present in the conventional reference antenna method and three-antenna method. In terms of the least-square method to determine  $A_0$ , the order selection of the regression polynomial, the number of measurement points, and antenna sweeping distance need to be reviewed carefully as the source of uncertainty.

Therefore, it should be noted that there may be a case where the use of extrapolation presents no merit — i.e. the uncertainty gained by assuming that the distance between antennas is already large enough is clearly smaller than that obtained using extrapolation technique. For example, in the case where STD and AUC are of the same shape, the use of extrapolation technique in the reference antenna method often provides little benefit.

### 7 Conclusion

In this paper, we reviewed methods applicable to actual gain calibration of two types of DRGA used in EMI measurement in frequencies larger than 1 GHz, and verifies that the two methods — the reference antenna method

with extrapolation technique and the three-antenna method with extrapolation technique — provide a way for practical DRGA calibration in a small semi-anechoic chamber with no need to cover its bare metallic floor.

Extrapolation technique proved to be an excellent tool that enables calibration without the need for a large measurement site, and eliminates the complicated problem of distance between antennas — i.e. from which part of the transmitting to which part of the receiving antenna should be defined as the distance between antennas. In certain cases, however, uncertainty resulting from extrapolation of distance characteristics curve (gained from antenna sweeping experiments) becomes so significant that it makes calibration without use of extrapolation technique a more favorable choice. The authors continue research toward quantitative evaluation of the uncertainty involved in extrapolating measured data, and to propose techniques applicable to DRGA calibration without the need for a large fully anechoic room. The authors are also planning to examine the technique's applicability to other types of antennas such as LPDA.

## Acknowledgment

A part of this work was financially supported by the research and development project for expansion of radio spectrum resources of the Ministry of Internal Affairs and Communications, Japan.

## References

- 1 Specification for radio disturbance and immunity measuring apparatus and methods - Part 2-3: Methods of measurement of disturbances and immunity - Radiated disturbance measurements, CISPR 16-2-3, Edition 3.0, 2010.
- 2 VCCI Council, Technical Requirements V-3/2015.04, Normative Annex 1, Rules for Voluntary Control Measures, April 2015.
- 3 L. H. Hemming and R. A. Heaton, "Antenna Gain Calibration on a Ground Reflection Range," *IEEE Trans. on Antennas and Propagation*, vol.AP-21, no.4, pp.532-538, July 1972.
- 4 K. Fujii, Y. Yamanaka, and A. Sugiura, "Antenna Calibration Using the 3-Antenna Method with the In-Phase Synthetic Method," *IEICE Trans. on Commun.* vol.E93-B, no.8, pp.2158-2164, Aug. 2010.
- 5 T. S. Chu and R. A. Sempak, "Gain of Electromagnetic Horns," *Bell Syst. Tech. J.* vol.44, pp.527-537, March 1965.
- 6 K. Fujii, S. Ishigami, and T. Iwasaki, "Evaluation of Complex Antenna Factor of Dipole Antenna by the Near-field 3-Antenna Method with the Method of Moment," *IEICE Trans. B-II*, vol.J79-B-2, no.11, pp.754-763, Nov. 1996. (in Japanese)
- 7 K. Harima, "Determination of gain of double-ridged guide horn antenna by considering phase center," *IEICE Electronics Express*, vol.7, no.2, pp.86-91, Jan. 2010.
- 8 K. Harima, "Accurate gain determination of LPDA by considering the phase center," *IEICE Electron. Express*, vol.7, no.23, pp.1760-1765, Dec. 2010.
- 9 K. Harima, "Numerical Simulation of Far-Field Gain Determination at Reduced Distances Using Phase Center," *IEICE Trans. Commun.*, vol.E97-B, no.10, pp.2001-2010, Oct. 2014.
- 10 A. C. Newell, R. C. Baird, P. F. Wacker, "Accurate Measurement of Antenna Gain and Polarization at Reduced Distances by an Extrapolation Technique," *IEEE Trans. on Antennas and Propagation*, AP-21, no.4, pp.418-431, July 1973.
- 11 IEICE, *Antenna Engineering Handbook*, 2nd edition, Ohmsha, July 2009. (in Japanese)
- 12 E.B. Larsen, R. L. Ehret D. G. Camell, and G. H. Koepke, "Calibration of Antenna Factor at a Ground Screen Field Site using an Automatic Network Analyzer," *IEEE 1989 National Symposium on Electromagnetic Compatibility*, pp.19-24, (Denver), May 1989.
- 13 S. Kaketa, K. Fujii, A. Sugiura, Y. Matsumoto, and Y. Yamanaka, "A Novel method for EMI antenna calibration on a metal ground plane," *IEEE International Symposium on EMC, MO-A-P1.8*, (Istanbul), May 2003.
- 14 M. Sakasai, H. Masuzawa, K. Fujii, A. Suzuki, K. Koike, and Y. Yamanaka, "Evaluation of Uncertainty of Horn Antenna Calibration with the Frequency range of 1 GHz to 18 GHz," *Journal of NICT*, vol.53, no.1, pp.29-42, March 2006.
- 15 T. Kitagawa, *Johoryo Tokeigaku, Kyoritsu Shuppan*, Jan. 1983. (in Japanese)
- 16 M. Ameya, M. Hirose, S. Kurokawa, "Uncertainty estimation of calibration system for V-band standard gain horn antenna using three-antenna extrapolation method," *IEICE Technical Report, ACT2010-09*, pp.7-12, Dec. 2010.
- 17 R. E. Borland, "The optimum range of separations for antenna gain measurement by extrapolation," *NPL Report DES 98*, Sept. 1990.
- 18 ISO, *Guide to the Expression of Uncertainty in Measurement*, 1st edition, 1995.



**Katsumi FUJII, Dr. Eng.**

Research Manager, Electromagnetic Compatibility Laboratory, Applied Electromagnetic Research Institute  
Calibration of Measuring Instruments and Antennas for Radio Equipment, Electromagnetic Compatibility



**Kojiro SAKAI**

Technical Expert, Electromagnetic Compatibility Laboratory, Applied Electromagnetic Research Institute  
Calibration of Measuring Instruments and Antennas for Radio Equipment



**Tsutomu SUGIYAMA**

Senior Researcher, Electromagnetic Compatibility Laboratory, Applied Electromagnetic Research Institute  
Calibration of Measuring Instruments and Antennas for Radio Equipment



**Kouichi SEBATA**

Senior Researcher, Electromagnetic  
Compatibility Laboratory, Applied  
Electromagnetic Research Institute  
Calibration of Measuring Instruments  
and Antennas for Radio Equipment,  
geodesy



**Iwao NISHIYAMA**

Electromagnetic Compatibility Laboratory,  
Applied Electromagnetic Research Institute  
Calibration of Measuring Instruments  
and Antennas for Radio Equipment